

Molecular Interactions between MASP-2, C4 and C2 and their activation fragments leading to complement activation via the lectin pathway*

Russell Wallis^{§§†}, Alister W. Dodds[†], Daniel A. Mitchell[#], Robert B. Sim[†], Kenneth B. M. Reid[†] and Wilhelm J. Schwaeble[‡]

From the Departments of [†]Infection, Immunity and Inflammation and [§]Biochemistry, University of Leicester, Leicester, UK, the [†]MRC Immunochemistry Unit, Department of Biochemistry, University of Oxford, Oxford, UK and the [#]Clinical Sciences Research Institute, University of Warwick, Coventry, UK

Running title: Interactions between MASP-2, C2 and C4

Address correspondence to: Russell Wallis, Department of Infection, Immunity and Inflammation, Medical Science Building, University of Leicester, University Road, Leicester, UK, Tel. +44 116 2231556; Fax. +44 116 2525030; E-Mail: rw73@le.ac.uk

Activation of component C3 is central to the pathways of complement and leads directly to neutralization of pathogens and stimulation of adaptive immune responses. The convertases that catalyse this reaction assemble from fragments of complement components via multistep reactions. In the lectin pathway, mannose-binding lectin (MBL) and ficolins bind to pathogens and activate MBL-associated serine protease-2 (MASP-2). MASP-2 cleaves C4, releasing C4a and generating C4b, which attaches covalently to the pathogen surface upon exposure of its reactive thioester. C2 binds to C4b and is also cleaved by MASP-2 to form the C3 convertase (C4b2a). To understand how this complex process is coordinated, we have analyzed the interactions between MASP-2, C4, C2 and their activation fragments and have compared MASP-2 catalyzed cleavage of C4b2 and C2. The data show that C2 binds tightly to C4b, but not to C4, implying that C4 and C2 do not circulate as pre-formed complexes, but that C2 is recruited only after prior activation of C4. Following cleavage of C4, C4b still binds to MASP-2 ($K_D \sim 0.6 \mu\text{M}$) and dissociates relatively slowly ($k_{off} \sim 0.06 \text{ s}^{-1}$) compared to the half-life of the thioester ($\leq 0.7 \text{ s}$, from Sepp, A. *et al. Protein Sci* 2, 706-716). We propose that the C4b-MASP-2 interaction favors attachment of C4b near to the activating MBL-MASP complex on the bacterial surface, so that following recruitment of C2, the proximity of enzyme and substrate (C4b2) combined with more favorable reaction kinetics, drive formation of the C3 convertase, promoting complement activation.

Complement is a fundamental part of the immune system, providing protection against invading microorganisms through both antibody-dependent and -independent mechanisms (1). It also mediates many cellular and humoral interactions within the immune response, including chemotaxis, phagocytosis, cell adhesion, and B-cell differentiation (2). Three different pathways initiate the complement cascade: the classical, alternative and lectin pathways (3). In the classical pathway, component C1q binds to a variety of targets including immune complexes to initiate the step-wise activation of associated serine proteases, C1r and C1s, thereby providing a major mechanism for pathogen clearance following engagement by the adaptive immune system. In the alternative pathway, spontaneous low-level hydrolysis of component C3 effects deposition of protein fragments onto cell surfaces, triggering complement activation on pathogens. While regulatory proteins on host tissues avert activation, preventing self-damage. In the lectin pathway (4,5) mannose-binding lectin (MBL¹) and serum ficolins bind directly to sugars or N-acetyl groups on pathogenic cells and activate MBL-associated serine proteases (MASPs) to initiate the complement cascade.

Three different MASPs (-1, -2 and -3) bind to MBL and ficolins (6-8). They are homologues of C1r and C1s of the classical pathway and comprise two CUB domains separated by a Ca^{2+} -binding EGF-like domain and followed by two CCP modules and a serine protease domain. MASPs normally circulate as zymogens bound to MBL and ficolins though their CUB and EGF-like domains (9). When the lectin components bind to a target cell, MASPs-1 and -2 activate through autolysis at a specific site within a linker region at the N-terminal end of

the serine protease domain. Only MASP-2 has a clearly defined role in complement activation. It initially cleaves C4 to produce the peptide anaphylatoxin C4a and the C4b fragment, which attaches to the cell surface. C2 then binds to C4b and is also cleaved by MASP-2 to generate C2b and C2a. C2a remains attached to C4b to become the catalytic component of the C3 convertase (C4b2a) (10,11). The roles of MASP-1 and MASP-3 are not known. MASP-1 cleaves C2 but not C4, so it might enhance complement activation triggered by lectin·MASP-2 complexes, but cannot initiate activation itself (12). MASP-3 does not autoactivate, so is probably activated through the action of an unknown protease (13). Its biological role and physiological substrates remain to be identified.

Recent studies have shown that MASP-2 forms extensive contacts with C4 during complement activation (12,14,15). Indeed, *in vitro*, zymogen MASP-2 interacts weakly with C4 through accessory-binding sites, even though the catalytic site is disrupted. These accessory sites, which probably include one or both of the CCP modules of the MASP, only become exposed upon activation of the MBL·MASP-2 complex, thereby enabling MASP-2 to bind to C4 (12). Additional changes at the catalytic site allow the MASP to cleave its substrates.

Complement activation must be tightly regulated to prevent tissue damage. Stable attachment of components to the surface of pathogens is one of the mechanisms employed by the host. MBL·MASP complexes bind tightly to pathogens through multivalent interactions between the carbohydrate-recognition domains of MBL and arrays of mannose-like sugars on cell surfaces (16). While analogous interactions between fibrinogen-like domains of ficolins and N-acetyl groups on pathogens immobilize ficolin·MASP complexes (17). When a lectin·MASP complex cleaves C4, the C4b fragment also attaches to the pathogen following exposure of a thioester, which reacts with the cell surface (18,19). For complement activation to proceed, the C4b fragment must be close enough to a lectin·MASP complex, so that the MASP can cleave C2 once it has bound to C4b. Control of this process is relatively poorly understood. Co-localization is probably achieved, in part, by the high reactivity of the thioester bond of C4b towards hydroxyl or amino groups on the pathogen surface.

Nevertheless, additional processes probably increase the efficiency of complement activation *in vivo*.

In this manuscript we have investigated the steps leading to C3 convertase formation by analyzing the molecular interactions between MASP-2, C4 and C2 and their activation fragments. Based on our findings, we propose a model to explain how interactions between MASP-2 and C4b coordinate the activation process following pathogen recognition.

Experimental Procedures

Materials - Tissue culture media were from Life Technologies. L-(tosylamido-2-phenyl) ethyl chloromethyl ketone-treated trypsin and phenylmethylsulphonyl fluoride were from Sigma.

Amino acid sequencing - Amino acid sequencing was carried out using an Applied Biosystems 494A Procise protein sequencer. Samples were run for 10 cycles using standard sequencing cycles.

Production of proteins and protein fragments - Recombinant proteins were used in these studies to ensure that preparations were not contaminated by trace amounts of other complement proteins. Previous work has demonstrated that components are processed correctly during biosynthesis and retain the key properties of native material (12,20).

Recombinant rat complement components C2 and C4 and catalytically active and inactive forms of rat MASP-2, called MASP-2K and MASP-2A, respectively, were produced by expression in Chinese hamster ovary cells and purified as described previously (12,20). MASP-2A comprises full-length MASP-2 in which the active site serine residue at position 613 is changed to an alanine. It was converted from the zymogen to the activated form by incubation with trypsin (0.25% w/w) for 1 hour at 37 °C in reaction buffer (50 mM Tris-Cl, pH 7.5, containing 150 mM NaCl) containing 1 mM CaCl₂ (Fig. 1). Edman degradation of the C-terminal fragment confirmed that cleavage occurred at the expected site for zymogen activation. Residual trypsin activity was inhibited by addition of phenylmethylsulphonyl fluoride (0.1 mg/ml final concentration) and protein was dialysed against reaction buffer to remove excess inhibitor. MASP-2K consists of full-length MASP-2 in which the arginine residue at the cleavage site for zymogen

activation (Arg⁴²⁴) is replaced by a lysine residue (12). This change reduces the rate of autocatalysis and thereby prevents activation of the zymogen during biosynthesis, secretion, and purification, allowing preparation of pure zymogen. MASP-2K was activated by incubation at 37 °C for 24 hours in reaction buffer containing 1 mM CaCl₂. Complement component C4b was generated from C4 by incubation with activated MASP-2K (0.02% w/w) for 1.5 hours at 37 °C, in reaction buffer (Fig. 1D). The reaction was stopped by addition of phenylmethylsulphonyl fluoride, as described above. Cleavage of all proteins was monitored by SDS-polyacrylamide gel electrophoresis and protein fragments were quantified by scanning gels using a Chemigenius bio-imaging system from Syngene. C4(met), in which the thioester has become exposed by reaction with methylamine, was produced by incubation of C4 with methylamine at pH 8 for 1 hour at 37 °C. Before further analysis, all proteins were dialysed against reaction buffer.

Proteolysis of the C4b2 complex - The catalytic activity of MASP-2K towards C4b2 was measured by incubating activated MASP-2K (1-2 nM) with increasing concentrations of C2 (0.1 – 2 µM) in the presence of excess C4b (2.5 µM), in reaction buffer containing 1 mM CaCl₂, 1 mM MgCl₂ and ovalbumin (40 µg/ml), at 37 °C. C2 and C4b were pre-incubated for 30 min before addition of enzyme to allow complex formation. At various times, aliquots were removed and the reaction was stopped by boiling in gel-loading buffer. The extent of C2 cleavage was determined by scanning SDS-polyacrylamide gels. To correct for minor differences in the amounts of sample loaded onto gels, values were normalized using the amount of ovalbumin in each aliquot as a reference. A similar assay was used to measure cleavage of C2, except that the concentration of activated MASP-2 was 1 nM and the concentration of C2 was between 1 and 10 µM. Initial rates were calculated from the first 10 % of cleavage or less. Data were fitted to the Michaelis-Menten equation by non-linear regression using the software Origin from Microcal.

Analytical ultracentrifugation - Equilibrium experiments were carried out as described previously in a Beckman XLA-70 centrifuge using epon charcoal-filled six-hole centrepieces (21,22). Before analysis, all proteins were dialysed extensively against

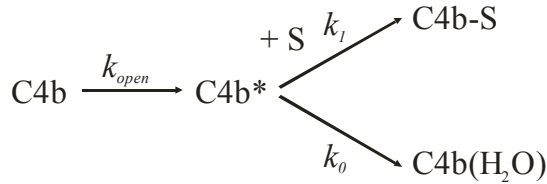
reaction buffer containing 1 mM CaCl₂ and 1 mM MgCl₂. To measure the interaction between activated MASP-2A and C4b, proteins were mixed at different molar ratios to give initial absorbances of 0.1 – 0.6 at 280 nm. Data were analyzed using the program 2C1SFIT, which implements conservation of mass constraints to model the equilibrium distributions globally (23). The apparent equilibrium association constant and the fraction of competent components were allowed to vary as global fitting parameters. Apparent equilibrium association constants were converted to molar dissociation constants as described (24). Values are mean ± S.E. from three independent experiments. It was assumed that no changes in the partial specific volumes occur on complex formation and that the molecular mass of the complex is the sum of that of the components. Molecular masses of MASP-2 and C4 were determined from experiments run in parallel (Table I), by fitting equilibrium data at three different loading concentrations to a model assuming a single solution species, using software supplied with the centrifuge.

Sedimentation velocity experiments were carried out at 40,000 rpm and at 20 °C using aluminium centrepieces. Prior to setting up the experiments, proteins were dialysed against reaction buffer containing 1 mM CaCl₂ and 1 mM MgCl₂. Scans were collected at 2 - 4 min intervals at 230 nm. Data were analyzed using the program DCDT (25). Values are displayed as $s_{20,w}$ (Table I) by correcting for the effects of buffers (26).

Surface plasmon resonance - Measurements were performed using a BIAcore 1000 instrument (BIAcore). Protein ligands were diluted to 25 µg/ml in 10 mM sodium acetate, pH 4.5 (C4, C4b and C4(met) or pH 3.5 or 4.0 (activated MASP-2A), and immobilized onto the carboxymethylated dextran surface of a CM5 sensor chip (BIAcore) using amine coupling chemistry (BIAcore amine coupling kit). Binding was measured in reaction buffer at a flow rate of 5 µl/min and at 25 °C. Regeneration of the protein surfaces between analyses was achieved by injection of 10 µl of 5 mM sodium acetate, pH 3.5, containing 1M NaCl. Data were analyzed by fitting to a 1:1 Langmuir binding model for several protein concentrations simultaneously, using BIAevaluation 3.1 software (BIAcore). The apparent equilibrium dissociation constants (K_D) were calculated from

the ratio of the dissociation and association rate constants ($k_{\text{off}}/k_{\text{on}}$).

Kinetics of C4 binding to substrate – Binding of C4b to a substrate S can be described by the following reaction scheme:



Measurements of C4 activation for a variety of species have been made using small substrates such as glycine and glycerol (27). Under pseudo-first order conditions, where $[\text{S}] \gg [\text{C4b}]$, the proportion of C4b binding to substrate is $[\text{S}] \cdot k_1 / k_0$. For human C4B, k_{open} is too rapid to measure. The pseudo-first order rate constant for hydrolysis, $k_0 (= k \cdot [\text{H}_2\text{O}]$, where k is the second order rate constant for hydrolysis), has been estimated as $\geq 1 \text{ s}^{-1}$ at 22°C ($t_{1/2} \leq 0.7 \text{ s}$). Thus, k_0 provides a lower limit for $[\text{S}] \cdot k_1$ assuming that at least equivalent amounts of C4b bind to substrate as are inactivated through hydrolysis.

RESULTS

Complement activation normally occurs on the surfaces of pathogens. Nevertheless, solution studies have provided key insights into the activation process. In this manuscript, we have adopted both solution and solid-phase approaches to study the molecular interactions leading to C3 convertase formation in the lectin pathway. Similar processes on the surfaces of pathogens probably help to regulate complement activation *in vivo*.

Recruitment of C2 by C4b - C2 binds to C4b with high affinity (28). However, binding between C2 and C4 has not been analyzed. Even a weak interaction between these components would probably facilitate C3 convertase formation, because both substrates would be present at the same time for their stepwise activation by a lectin·MASP-2 complex. We therefore examined whether C4 binds to C2. Freshly prepared C4 was used in these experiments to minimize hydrolysis of the thioester, which occurs spontaneously in solution but at a low rate. This precaution was necessary because thioester-hydrolyzed, but peptide-bond intact C4 binds to C2 and the resulting

complexes would have similar properties to C4b2 complexes. Samples, at concentrations comparable to those that occur *in vivo*, were analyzed by velocity analytical ultracentrifugation, using the time derivative method $g(s^*)$ to display the distribution of apparent sedimentation coefficients (s^*). Using this approach, complexes can be distinguished from free components by differences in the rates at which they sediment. In a mixture of C2 and C4, the s^* distribution corresponded closely to the sum of the distributions of the components analysed separately (Fig. 2A), indicating that C2 and C4 do not interact with each other over the range of concentrations examined. By contrast, when C4b was mixed with C2, a new peak was observed corresponding to a complex, which sedimented faster than either of the free components, confirming that C4b binds to C2 (Fig. 2B). Only small amounts of un-associated species were detected in the mixture indicating that the K_D of the C4b2 complex is considerably lower than the loading concentration of the components ($0.2 \mu\text{M}$), consistent with previous studies in which the K_D for the interaction between human C4b and C2 was determined as $\sim 1 \times 10^{-8} \text{ M}$ (28). Thus, we conclude that C2 and C4 do not interact with each other before activation of C4. However, following cleavage of C4, C2 binds tightly to C4b to form the C4b2 complex, which is subsequently cleaved again to form the C3 convertase.

Interactions between activated MASP-2 and C4b - Binding between MASP-2 and C4b, following activation of C4, would help to ensure that C4b attaches to the pathogen surface close to the lectin·MASP-2 complex. Co-localization of these components, in turn, would increase the probability of cleavage of the C4b2 complex by the same MASP and would thus help to coordinate C3 convertase formation. Following cleavage of C4, the C4b fragment undergoes a conformational change which exposes the thioester. Nevertheless, at least some of the MASP-binding sites might still remain after the conformational change. To examine this possibility, we tested whether MASP-2 binds to C4b. In a mixture of activated MASP-2A and C4b, the amount of unassociated MASP-2 decreased and the average s^* increased relative to the individual components measured separately, indicating that MASP-2A does indeed bind to C4b (Fig. 3). Some of the MASP was still unassociated in the mixture, so the K_D is

probably greater than the loading concentration of the components (0.4 μM).

To investigate binding between MASP-2A and C4b further, samples were analyzed by equilibrium ultracentrifugation. In a mixture of both components, more protein was distributed toward the bottom of the cell compared to the sum of the equilibrium distributions of the components, confirming the presence of MASP-2A·C4b complexes (Fig. 4A). The strength of the interaction was quantified by comparing mixtures of MASP-2A and C4b at different molar ratios. Data from three separate experiments, each at two different loading concentrations, fitted well to models assuming formation of 1:1 complexes, in which the K_D was $2.7 \pm 1.3 \mu\text{M}$ (Fig. 4B).

Interestingly, the affinity of the interaction between activated MASP-2A and C4b is comparable with the affinity between zymogen MASP-2 and intact C4, characterised previously under comparable conditions ($6.8 \pm 2.0 \mu\text{M}$) (12,14). The latter interaction is mediated through accessory-binding sites on the MASP, which become exposed following activation of the MBL·MASP complex, thereby lowering the K_M for catalysis of C4. Given their comparable affinities, it is likely that MASP-2 binds to C4 and C4b through the same binding sites, implying that the binding surface is maintained upon cleavage of C4, despite the subsequent conformational change.

While the affinity of the interaction between activated MASP-2 and C4b is relatively low compared to many protein-protein interactions (e.g. binding between C4b and C2), it is unusually high for an enzyme-product complex, where affinities are often in the mM range. Binding between enzyme and product might help to localize C4b near the lectin·MASP-2 complex on the pathogen by trapping the C4b molecule until it has attached covalently to the cell surface. The probability of such a process is dependent on the relative magnitudes of the rate of dissociation of C4b from MASP-2 (k_{off}) following cleavage of C4 and the rates at which the thioester is exposed and subsequently reacts with its substrate (see Experimental procedures). If dissociation is of a similar magnitude or slower than the reactivity of the thioester, a significant proportion of C4b molecules are likely to bind covalently to

hydroxyl or amino groups on the cell surface before their release by the enzyme.

To analyse the kinetics of the interaction between C4b and MASP-2, each component was immobilized in turn and binding by its soluble partner was measured using surface plasmon resonance. Data for MASP-2A binding to immobilized C4b are shown in Figure 5A and the kinetic parameters from all experiments are summarized in Table II. Reassuringly, the association (k_{on}) and dissociation (k_{off}) rate constants were comparable irrespective of whether MASP-2A or C4b was attached to the sensor chip. Furthermore, the K_D s (at 25 °C; calculated from k_{off}/k_{on}) were broadly comparable to the K_D measured by equilibrium ultracentrifugation (at 20 °C), demonstrating that immobilization of either component did not impair binding greatly. The k_{off} values were $7.4 \pm 4 \times 10^{-2}$ ($t_{1/2} = 11.5 \pm 4.8$ s) and $4.6 \pm 1.4 \times 10^{-2}$ s⁻¹ ($t_{1/2} = 16.7 \pm 5.1$ s) using immobilized C4b and MASP-2A, respectively. By comparison, the half-life of the thioester in human C4B (see *Kinetics of C4 binding to substrate*, above) is ≤ 0.7 s (27). So assuming that the activation kinetics of rat C4 are broadly comparable to those of human C4B, then a significant proportion of C4b molecules are likely to bind to substrate before release from the MASP. Thus, the relatively slow dissociation of C4b from MASP-2 probably helps to co-localise these components on an activating surface, thereby enabling subsequent cleavage of C2 by the same MASP.

To further probe the activation mechanism, we also measured the interactions of MASP-2A with C4 and with C4(met) (Fig. 5 and Table II). MASP-2A bound to C4 4- to 10-fold more tightly than to C4b, probably due to additional contacts between enzyme and substrate at or near the active site. Interestingly, very little binding was detected between MASP-2A and C4(met), even though the amount of C4(met) bound to the sensor chip was comparable to the amounts of C4 and C4b (Fig. 5C). Likewise, only minimal binding was detected between soluble C4(met) and immobilized MASP-2A at concentrations of C4(met) up to 0.5 μM . We conclude that MASP-2 binds more weakly to C4(met) than to C4b, despite both proteins undergoing similar conformational changes upon cleavage of the thioester. The most likely explanation for this observation is that the C4a fragment, which is

still covalently attached in C4(met) but not in C4b, impairs MASP-2 binding.

Catalysis of the C4b2 complex by MASP-2 - During formation of the C3 convertase, C4b, the product of the first MASP-2 catalyzed reaction, becomes part of the substrate of the second reaction (C4b2). Any persisting interactions between the MASP and the C4b component of C4b2 would be likely to affect the reaction kinetics. In order to investigate the role of C4b in cleavage of C4b2, we compared the cleavage of C4b2 with cleavage of C2 alone. Kinetic parameters are shown in Table III and examples of cleavage of C4b2 and C2 by MASP-2K on polyacrylamide gels are shown in Figure 6. Both reactions followed Michaelis-Menten kinetics over the concentration ranges examined. There is a modest increase in the catalytic efficiency of C4b2 cleavage compared to C2 cleavage, which is characterised by a 7-fold lower K_M and a smaller reduction in k_{cat} (Table III). Thus, C4b binding modifies the kinetics of C2 cleavage catalysed by MASP-2. The significance of these findings are discussed below.

DISCUSSION

The data presented here suggest novel mechanisms for regulation of C3 convertase formation during complement activation by the lectin pathway. By combining these findings with existing knowledge, we revise the current model for the early stages of complement activation (Fig. 7): when MBL-MASP-2 or ficolin-MASP-2 complexes bind to the surface of a pathogen, conformational changes trigger MASP autoactivation. Activated MASP-2 binds to C4 through accessory-binding sites on the CCP domains as well as at the active site within the protease domain, leading to cleavage of the C4 polypeptide (12). The newly exposed thioester on C4b reacts with hydroxyl or amino groups on the bacterial cell surface before dissociation from the MASP, thus binding proximal to the activating lectin-MASP-2 complex. Co-localization of these components facilitates subsequent cleavage of incoming C2 molecules by the same MASP, thereby coordinating activation.

Intriguing questions still remain concerning the order of events during the initial stages of complement activation. For example, it is uncertain whether C4a is released from C4b

immediately after cleavage by the lectin-MASP complex (as shown in Figure 7) or at a later stage. Interestingly, during C3 activation, C3a remains associated with C3b and may not be released until the larger C3b fragment is broken down to iC3b (29).

It is important to acknowledge that complement activation normally occurs on the surfaces of foreign cells in serum, which is a very different environment from those typically used for *in vitro* studies. *In vivo*, activation is controlled by a variety of regulators and inhibitors and many different serum proteins and carbohydrates interact with components to modulate the process. For example, in the classical pathway, C1 inhibitor plays a major role in the activation efficiency of C1s, the classical pathway homolog of MASP-2 by binding and inhibiting C1 and the subsequent activation of C2 and C4 (30). C1 inhibitor also binds and inhibits MASP-2 (11), so might play a comparable role in the lectin pathway, although the kinetics of the interaction have not been examined. The fate of activating MBL-MASP complexes on a cell surface is thus likely to depend on the relative rates of recruitment of substrates compared to binding by C1 inhibitor as well as to the influences of other regulators. In the classical pathway it has been estimated that only 35 C4 molecules and four C2 molecules are activated for each activating C1 complex, due to inhibition by C1 inhibitor (30). Nevertheless this rate of turnover is sufficient to trigger activation, which is subsequently amplified further by latter steps in the reaction cascade.

Complement is also regulated by polysaccharides, such as heparin and heparan sulphate, which bind to many complement components, including C4, C1 inhibitor and more weakly to C2 (31). While these and other protein-protein or protein-carbohydrate interactions might modulate enzyme activities or compete for substrate binding, they are unlikely to change the underlying activation mechanism proposed here, because the key step of C4b deposition onto the activating surface (such as a bacterial cell wall) is faster than its release from MASP-2 and therefore happens while C4b is still attached to the enzyme.

It is relatively unusual for the product of an enzyme-catalyzed reaction to bind to its enzyme with appreciable affinity, because such interactions are likely to reduce the efficiency of

catalysis by blocking the catalytic site. During formation of the C3 convertase, however, interactions between the product of the first reaction (C4b) and the enzyme (MASP-2) probably help to coordinate the two-step reaction on the pathogen surface by reducing the probability of additional C4 cleavage while increasing the chances of C4b2 cleavage. In addition, the proximity of C4b2 and MASP-2 will increase the effective concentration of substrate (C4b2) greatly, thus driving formation of the convertase.

Interestingly, while the K_M for C2 cleavage decreases by 7-fold when C4b binds to C2, the increase in the catalytic efficiency of the reaction in solution is relatively modest (~ 2 fold). As discussed above, on the surface of a bacterial cell cleavage of C4b2 is likely to be driven by its high effective concentration. Nevertheless, it is interesting to consider the kinetics of the reaction in solution and the changes that occur when C2 binds to C4b. Cleavage of C4 and C4b2 by MASP-2 are both characterized by relatively low K_M values, which for C4 at least is due to a relatively low K_D for the enzyme-substrate complex. Generally, a relatively stable enzyme-substrate complex is likely to improve substrate specificity but at the expense of catalysis (because of the increase in the resulting energy barrier). However, such properties might be advantageous in the complement cascade where control of activation is particularly important. The data would be consistent with this model, in which a decrease in the K_M for C4b2 cleavage compared to C2 cleavage alone is partially offset by a corresponding decrease in k_{cat} . An alternative explanation for the differences in catalysis of C4b2 and C2 is that binding to C4b induces a conformational change in C2. Indeed, a similar explanation has been proposed in the classical pathway for cleavage of C4b-bound C2 by C1s.

Once cleavage of the C4b2 complex is complete, the MASP will be free for subsequent rounds of catalysis. Consequently, activation probably results in each lectin-MASP-2 complex becoming surrounded by multiple C3 convertase complexes. Because substrates, inhibitors and regulators must bind to activating complexes, steric factors might affect complement activation *in vivo*. As more proteins are deposited onto the surface, further access might become blocked. Consequently, any C4b molecules that attach to the pathogen surface further away from the

initiating lectin-MASP-2 complex can still bind to C2, but are less likely to be converted to C4b2a complexes, because the MASP is not close enough to catalyse the second step of the reaction. Under these circumstances, C4b2 cleavage will only occur if another lectin-MASP complex binds close enough to catalyse the reaction.

An important assumption that we have made in our analysis is that the kinetics of rat C4 activation and substrate binding are similar to those of human C4B. It is important to consider whether this assumption is likely to be valid. Comparison of the reactivities of C4 isolated from a variety of species has shown that rat C4, like human C4B and most other mammalian C4s, has a preference for hydroxyl groups as substrates, while C4A is more reactive towards amino and thiol groups (32). These differences are due largely to a single amino acid difference at position 1106 (His in C4B and rat C4 and Asp in C4A) (33). The relative reactivities ($k_{1rat} \cdot k_{0C4B} / k_{0rat} \cdot k_{1C4B}$) of rat C4 and human C4B are 1.12 and 1.24 using glycine and glycerol as substrates (32). Thus, although absolute rate constants for rat C4 have not been determined, it is likely that the kinetics are similar to those of human C4B. It is also worth noting that in our analysis, we have used the rate of hydrolysis of C4B as a measure of the half-life of the thioester. On the surface of a bacterial cell, the effective concentrations of the more reactive hydroxyl and amino groups are likely to be extremely high, so the half-life of the thioester is probably much shorter.

The C3 convertase of the classical pathway is formed by a mechanism similar to that in the lectin pathway, although in this case C1s catalyses cleavage of C4 and C2. Formation of the C3 convertase might be regulated in a manner similar to that for the lectin pathway. Indeed, analysis of classical pathway activation has revealed that accessory-binding sites, probably located within the CCP modules of C1s, also facilitate recognition of C4, in a manner analogous to those between MASP-2 and C4 (34). Interestingly, however, although C1s and MASP-2 share the same substrates, binding through the protease domains of the enzymes is achieved through different enzyme-substrate contacts (35). Likewise, the CCP modules of MASP-2 have a higher C4-recognition efficacy than the equivalent domains of C1s, implying that there are additional differences in contacts

between the two systems (15). Thus, it will be very interesting to examine classical pathway activation, to reveal if mechanisms similar to those described here help to coordinate C3 convertase formation.

REFERENCES

1. Porter, R. R., and Reid, K. B. M. (1978) *Nature* 275, 699-704
2. Carroll, M. C. (2004) *Nat Immunol* 5(10), 981-986
3. Whaley, K., and Schwaeble, W. (1997) *Semin Liver Dis* 17(4), 297-310
4. Schwaeble, W., Dahl, M., Thiel, S., Stover, C., and Jensenius, J. (2002) *Immunobiology* 205, 455-466
5. Turner, M. W. (1996) *Immunology Today* 17, 532-540
6. Dahl, M. D., Thiel, S., Matsushita, M., Fujita, T., Willis, A. C., Christensen, T., Vorup-Jensen, T., and Jensenius, J. C. (2001) *Immunity* 15, 127-135
7. Sato, T., Endo, Y., Matsushita, M., and Fujita, T. (1994) *International Immunology* 6, 665-669
8. Thiel, S., Vorup-Jensen, T., Stover, C. M., Schwaeble, W., Laursen, S. B., Poulsen, K., Willis, A. C., Eggleton, P., Hansen, S., Holmskov, U., Reid, K. B. M., and Jensenius, J. C. (1997) *Nature* 386, 506-510
9. Wallis, R., and Dodd, R. B. (2000) *J Biol Chem* 275(40), 30962-30969
10. Kerr, M. A. (1980) *Biochem J* 189(1), 173-181
11. Rossi, V., Cseh, S., Bally, I., Thielens, N. M., Jensenius, J. C., and Arlaud, G. J. (2001) *J Biol Chem* 276(44), 40880-40887
12. Chen, C. B., and Wallis, R. (2004) *J Biol Chem* 279(25), 26058-26065
13. Zundel, S., Cseh, S., Lacroix, M., Dahl, M. R., Matsushita, M., Andrieu, J. P., Schwaeble, W. J., Jensenius, J. C., Fujita, T., Arlaud, G. J., and Thielens, N. M. (2004) *J Immunol* 172(7), 4342-4350
14. Gal, P., Harmat, V., Kocsis, A., Bian, T., Barna, L., Ambrus, G., Vegh, B., Balczer, J., Sim, R. B., Naray-Szabo, G., and Zavodszky, P. (2005) *J Biol Chem* 280(39), 33435-33444
15. Rossi, V., Teillet, F., Thielens, N. M., Bally, I., and Arlaud, G. J. (2005) *J Biol Chem* 280(51), 41811-41818
16. Weis, W. I., and Drickamer, K. (1994) *Structure* 2, 1227-1240
17. Matsushita, M., Endo, Y., and Fujita, T. (2000) *J Immunol* 164(5), 2281-2284
18. Law, S. K., and Dodds, A. W. (1997) *Protein Sci* 6(2), 263-274
19. Møller-Kristensen, M., Thiel, S., Hansen, A. G., and Jensenius, J. C. (2003) *Scandinavian J Immunol* 57, 556-561
20. Chen, C. B., and Wallis, R. (2001) *J Biol Chem* 276(28), 25894-25902
21. Wallis, R., and Drickamer, K. (1997) *Biochem J* 325 (Pt 2), 391-400
22. Wallis, R., and Drickamer, K. (1999) *J Biol Chem* 274(6), 3580-3589
23. Minton, A. P. (1997) *Progress in Colloid and Polymer Science* 107, 11-19
24. Rivas, G., Stafford, W., and Minton, A. P. (1999) *Methods* 19, 194-212
25. Stafford, W. F. (1992) *Analytical Biochemistry* 203, 295-301
26. Laue, T. M., Bhairavi, D. S., Ridgeway, T. M., and Pelletier, S. L. (1992). In: Harding, S. E., Rowe, A. J., and Horton, J. C. (eds). *Analytical Ultracentrifugation in Biochemistry and Polymers Science*, Royal Society of Chemistry
27. Sepp, A., Dodds, A. W., Anderson, M. J., Campbell, R. D., Willis, A. C., and Law, S. K. (1993) *Protein Sci* 2(5), 706-716
28. Laich, A., and Sim, R. B. (2001) *Biochim Biophys Acta* 1544(1-2), 96-112
29. Janatova, J., Tack, B. F., and Prahl, J. W. (1980) *Biochemistry* 19(19), 4479-4485
30. Ziccardi, R. J. (1981) *J Immunol* 126(5), 1769-1773
31. Yu, H., Munoz, E. M., Edens, R. E., and Linhardt, R. J. (2005) *Biochim Biophys Acta* 1726(2), 168-176
32. Dodds, A. W., and Law, S. K. (1990) *Biochem J* 265(2), 495-502
33. Dodds, A. W., Ren, X. D., Willis, A. C., and Law, S. K. (1996) *Nature* 379(6561), 177-179
34. Rossi, V., Bally, I., Thielens, N. M., Esser, A. F., and Arlaud, G. J. (1998) *J. Biol. Chem.* 273(2), 1232-1239

35. Harmat, V., Gal, P., Kardos, J., Szilagy, K., Ambrus, G., Vegh, B., Naray-Szabo, G., and Zavodszky, P. (2004) *J Mol Biol* 342(5), 1533-1546

FOOTNOTES

This work was supported by grants from the Wellcome Trust (077400 to RW and WS and 060574 to WS). The analytical ultracentrifugation facility at Oxford was set up using grants from the BBSRC and Wellcome Trust. RW and DM are RCUK Academic Fellows.

¹The abbreviations used are: MBL, mannose-binding lectin; MASP, MBL-associated serine protease; CUB domain, domain found in complement component C1r/C1s, Uegf, and bone morphogenic protein 1; EGF, epidermal growth factor; CCP, complement control protein; C4(met), C4 in which the thioester has become exposed by reaction with methylamine.

FIGURE LEGENDS

Fig. 1. *A and B*, Domain organisations of rat MASP-2 and C4. *Balls on sticks* show the positions of N-linked glycosylation sites. Disulfide bonds that link polypeptide chains are shown by *solid lines*. *C*, SDS-polyacrylamide gel electrophoresis of zymogen and activated MASP-2A. MASP-2A was converted from the zymogen to the activated conformation by limited digestion with trypsin. Proteins were separated on a 12% gel under reducing conditions and were detected by staining with Coomassie blue. Edman degradation of the smaller, C-terminal fragment gave the sequence IIGGQPAKPG, confirming that cleavage occurred at the expected site for activation (12). The C-terminal fragment migrates as two bands on the gel due to differential glycosylation. *D*, SDS-polyacrylamide gel electrophoresis of C4 and C4b. C4b was generated by digestion of purified C4 with activated MASP-2K. Proteins were separated on a 10% gel under reducing conditions and detected by staining with Coomassie Blue.

Fig. 2. Sedimentation analytical ultracentrifugation analysis of mixtures of *A*, C2 (0.25 μM) with C4 (0.20 μM) and *B*, C2 (0.2 μM) with C4b (0.2 μM). The $g(s^*)$ distribution of each component was determined from separate experiments run in parallel at identical protein concentrations. The dotted lines represents the predicted $g(s^*)$ distributions assuming no interactions.

Fig. 3. Sedimentation velocity analysis of activated MASP-2A and C4b. MASP-2A, the catalytically inactive form of MASP-2, was used to prevent non-specific proteolysis during the course of the experiment. Prior to setting up the run, it was converted from the zymogen to the activated conformation by limited digestion with trypsin. Loading concentrations of activated MASP-2A and C4b were 0.65 and 0.4 μM , respectively. The sum of the $g(s^*)$ distributions of the individual components, representing the predicted $g(s^*)$ assuming no interaction, is shown by the dotted line.

Fig. 4. Interaction between activated MASP-2A and C4b by equilibrium analytical ultracentrifugation. *A*, Loading concentrations of activated MASP-2A and C4b were 0.35 μM . Equilibrium distributions were measured at 8000 rpm and 20 °C. The dotted line is the sum of the equilibrium distributions of the individual components analysed separately at identical protein concentrations and represents the predicted distribution assuming no interaction. *Top*, the difference between the equilibrium distribution of the mixture of activated MASP-2A and C4b and the sum of the equilibrium distributions of the individual components. The bar to the left of the plot represents 0.04 A_{234} units. Error bars represent the sums of the errors of the distributions of individual components and of the mixture, from five absorbance measurements. *B*, Loading concentrations were 1.53 μM C4 and 1.01 μM MASP-2A (\circ) and 1.04 μM C4 and 1.3 μM MASP-2A (\square). Solid lines represent the best fit to a model in which 1:1 complexes of C4 and activated MASP-2A are in equilibrium with the free components. The residuals for this model are shown together with the residuals for a model in which there is no interaction. The sums of the squares of the residuals were 0.0032 for the 1:1 binding model and 0.023 for a model in which there is no interaction. Bars to the right of the residual plots

represent 0.02 A_{280} units. Incorporation of additional parameters in to the fitting procedure did not improve the fit significantly, indicating that the proteins do not form larger complexes under the conditions tested.

Fig. 5. Analysis of the interactions of activated MASP-2A with immobilized C4b, C4 and C4(met) using surface plasmon resonance. Comparable amounts of C4 and its derivatives (between 8500 and 9000 response units were immobilized on separate channels of the same sensor chip. MASP-2A was injected at concentrations ranging from 0.4 μM to 6.3 nM. Only certain binding curves are shown for clarity. *A*, interaction with C4b. Concentrations of MASP-2A were 0.4, 0.2, 0.1, 0.05 and 0.025 μM . *Inset*, Scatchard plot of MASP-2A binding to immobilized C4b. Binding reached a plateau during the course of each injection, implying that equilibrium was reached. The amount of MASP-2A bound at equilibrium (in response units) was determined from the magnitude of the plateau. The K_D was 0.47 ± 0.13 μM based on combined data from two separate experiments. *B*, interaction with C4. Concentrations of MASP-2A were 0.2, 0.1, 0.05, 0.025 and 0.125 μM . *C*, interaction with C4(met). Concentrations of MASP-2A were as in *A*.

Fig. 6. Cleavage of C4b2 complexes and C2 by MASP-2K analysed by SDS-polyacrylamide gel electrophoresis. Ovalbumin (0.6 μg in each lane) was included in the reaction mixtures to prevent non-specific interactions and to correct for minor differences in the amounts of protein loaded on to gels. Proteins were detected with Coomassie blue. *A*, C2 (1.5 μM) with an excess of C4b (2.5 μM) was incubated with activated MASP-2K (2 nM) at 37 $^{\circ}\text{C}$. Aliquots were removed and proteins were separated on a 12 % polyacrylamide gel. Gel electrophoresis was carried out under non-reducing conditions, so that the cleavage products (C2a and C2b fragments) could be distinguished from the three C4b polypeptides. *B*, C2 (10 μM) was incubated with activated MASP-2K (1 nM) at 37 $^{\circ}\text{C}$. Proteins were separated on a 15% gel, under reducing conditions. Only the initial rates were measured.

Fig. 7. Model of C3 convertase formation in the lectin pathway of complement. *A*, Binding to the surface of a pathogen induces autoactivation of MBP-MASP-2, exposing accessory C4-binding sites on the MASP and leading to recruitment of C4. *B*, MASP-2 cleaves C4. Anaphylatoxin C4a, is released, while interactions between the MASP and the C4b fragment lead to covalent attachment of C4b proximal to the activating lectin-MASP-2 complex on the pathogen surface. *C*, C2 binds to C4b and the resulting complex is cleaved by the same MASP-2 molecule to form the C3 convertase (C4b2a). *D*, C2b probably remains attached to the convertase through non-covalent interactions (10). Proteins are represented in schematic form for simplicity.

TABLE I

Biophysical properties of complement components

Unmodified molecular masses and partial specific volumes of proteins were calculated from their amino acid compositions (26). Weight averaged molecular masses were determined by equilibrium ultracentrifugation. ^aData from (12)

Protein	Unmodified monomer molecular mass	Partial specific volume	Sedimentation coefficient ($s_{20,w}$)	Weight-averaged molecular mass
	<i>kDa</i>	<i>ml/g</i>	<i>S</i>	<i>kDa</i>
MASP-2A	74.8	0.722	5.50 ± 0.02	139 ± 1
C2	83.2	0.730	5.35 ± 0.04	N.D.
C4	190.0	0.732	8.01 ± 0.02	200 ^a
C4b	181.6	0.732	7.31 ± 0.16	187 ± 4

Table II

Kinetic properties of the interactions between C4 and C4b with activated MASP-2A^a

Immobilized Protein	Soluble Protein	k_{on}^b	k_{off}^b	K_D
		($M^{-1} s^{-1}$)	(s^{-1})	(μM)
C4b	MASP-2A	$1.9 \pm 0.3 \times 10^5$	$7.4 \pm 4 \times 10^{-2}$	0.5 ± 0.3
C4	MASP-2A	$4.7 \pm 0.7 \times 10^5$	$0.7 \pm 0.2 \times 10^{-2}$	0.05 ± 0.03
MASP-2A	C4b	$1.2 \pm 0.5 \times 10^5$	$4.6 \pm 1.4 \times 10^{-2}$	0.7 ± 0.3
MASP-2A	C4	$3.4 \pm 0.7 \times 10^5$	$2.3 \pm 0.5 \times 10^{-2}$	0.19 ± 0.07

^ainteractions between C4(met) and activated MASP-2A were not quantifiable to the weakness of binding

^bmean value determined from two separate experiments

Table III

Kinetic properties of activated MASP-2K with protein substrates

Substrate	K_M	k_{cat}	k_{cat}/K_M
	(μM)	(s^{-1})	($\mu M^{-1} s^{-1}$)
C2	5.1 ± 0.6	3.9 ± 1.6	0.85 ± 0.42
C4b2	0.72 ± 0.07	1.1 ± 0.3	2.0 ± 0.2

Figure 1

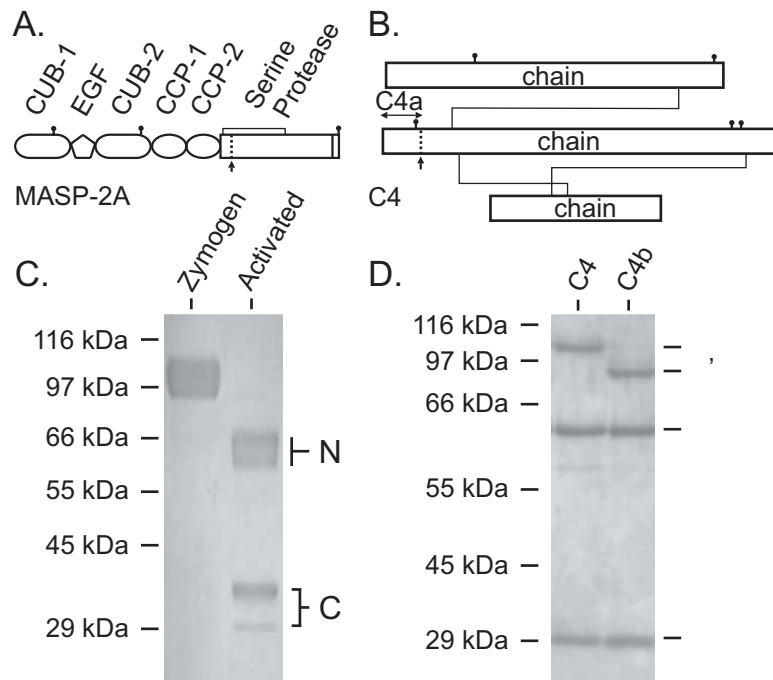


Figure 2

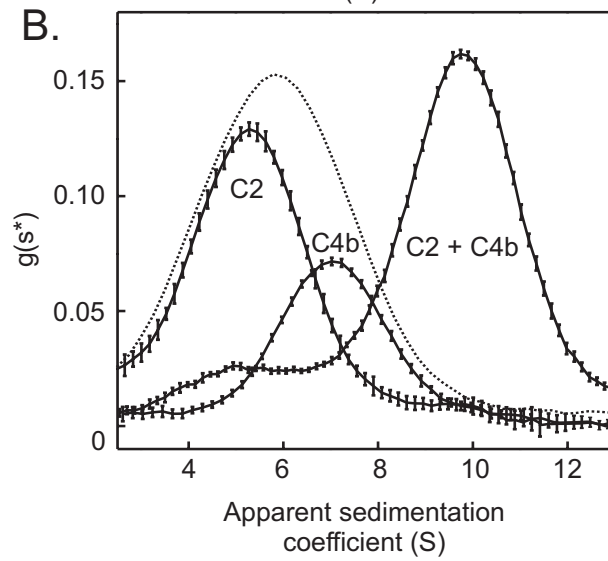
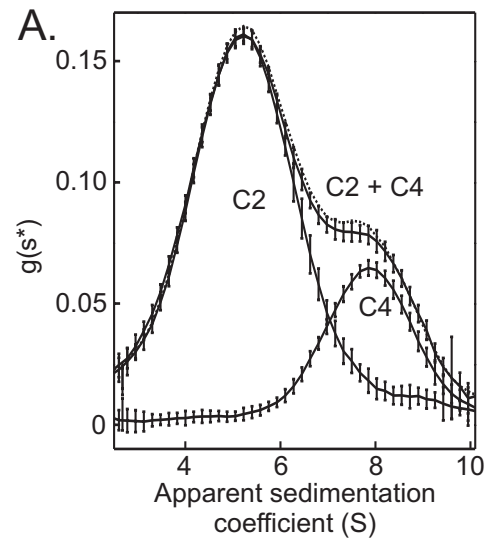


Figure 3

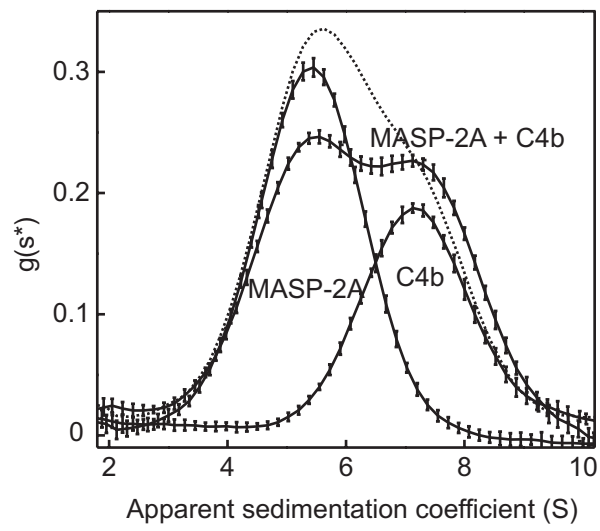


Figure 4

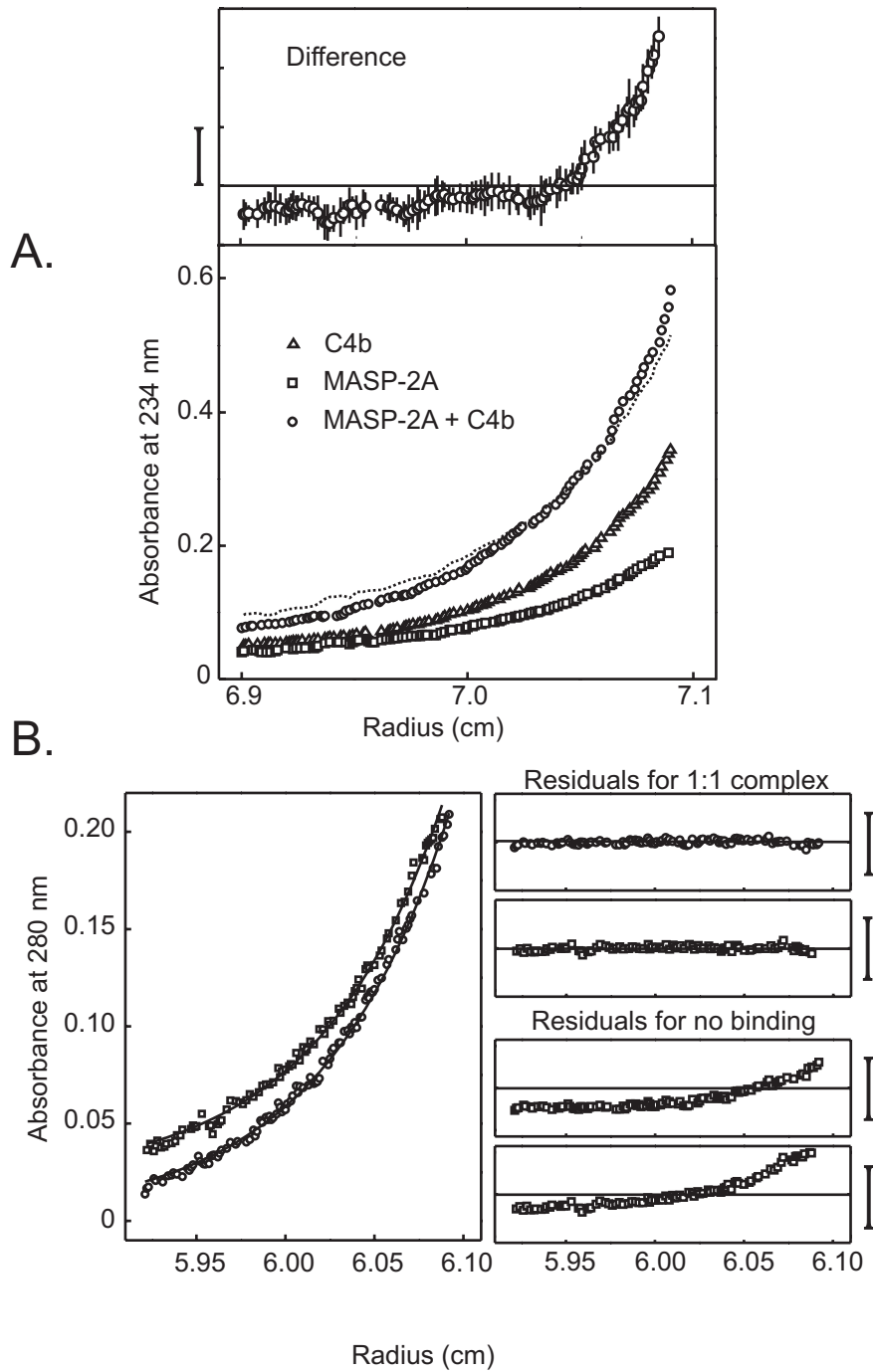


Figure 5

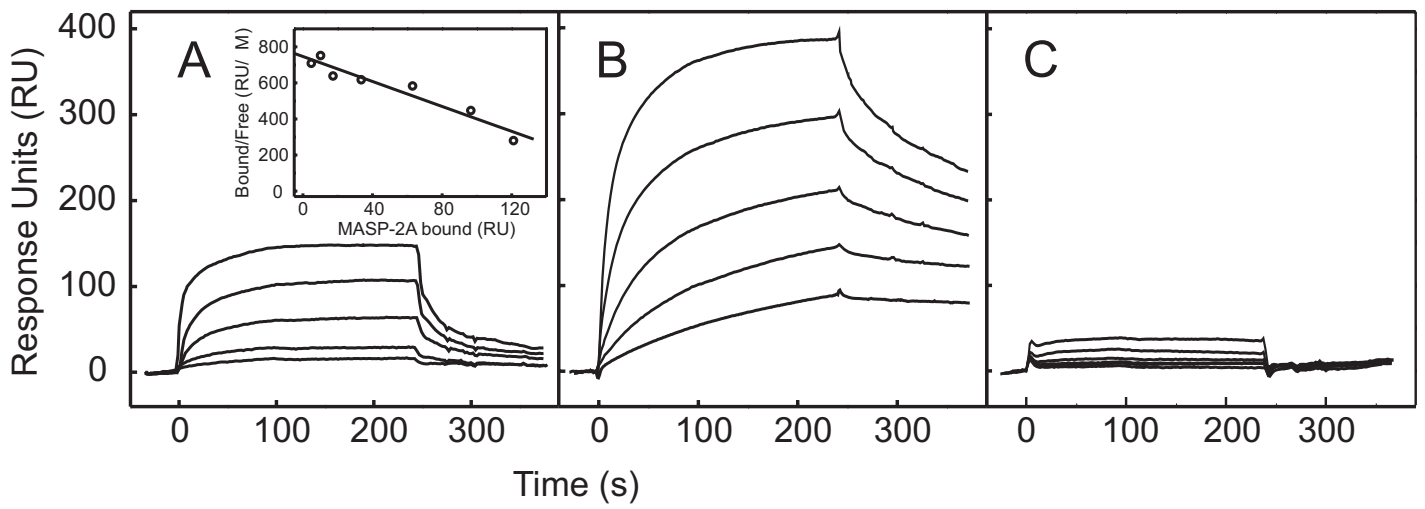


Figure 6

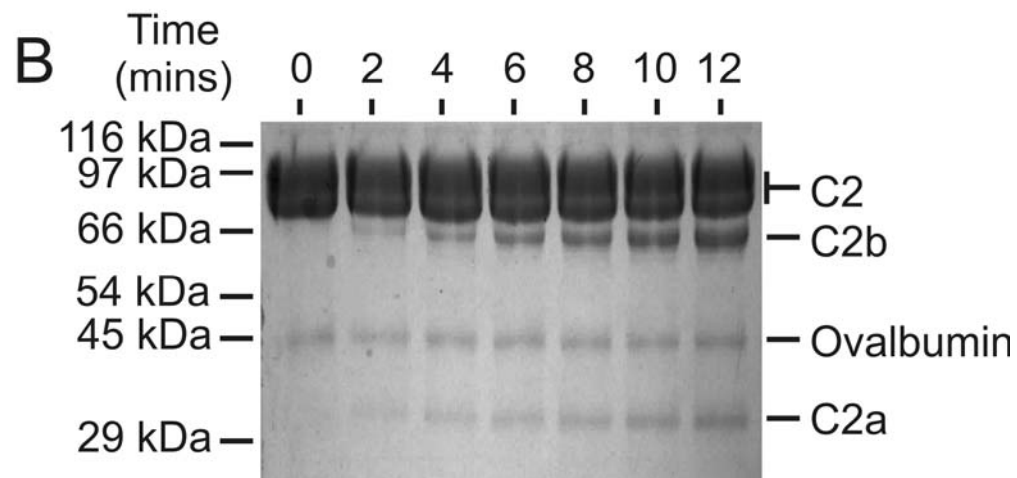
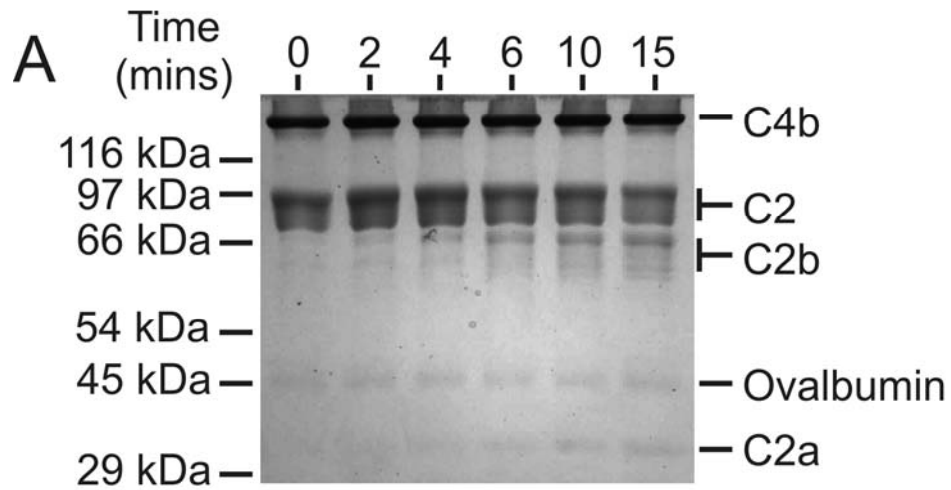


Figure 7

